ACS OMEGA

http://pubs.acs.org/journal/acsodf

Article

Self-Assembling pH-Responsive Nanoparticle Platform Based on Pectin−Doxorubicin Conjugates for Codelivery of Anticancer Drugs

Yinghua Tao, Dan Zheng, Jingyang Zhao, Kefeng Liu, Jing Liu, Jiandu Lei,* and Luying Wang*

Cite This: *ACS Omega* 2021, 6, 9998−10004

Read Online

ACCESS | Metrics & More | Article Recommendations | Supporting Information

ABSTRACT: Pharmaceutical science based on biological nanotechnology is developing rapidly in parallel with the development of nanomaterials and nanotechnology in general. Pectin is a natural polysaccharide obtainable from a wide range of sources. Here, we show that doxorubicin (DOX)-conjugated hydrophilic pectin (PET) comprising an amphiphilic polymer loaded with hydrophobic dihydroartemisinin (DHA) self-assemble into nanoparticles. Importantly, conjugated DOX and DHA could be released quickly in a weakly acidic environment by cleavage of the acid-sensitive acyl hydrazone bond. Confocal microscopy and flow cytometry confirmed that these PET-DOX/DHA nanoparticles efficiently delivered DOX into the nuclei of MCF-7 cells. Significant tumor growth reduction was monitored in a female C57BL/6 mouse model, showing that the PET-DOX/DHA nanoparticle-mediated drug delivery system inhibited tumor growth and may improve therapy. Thus, we have demonstrated that pectin may be useful in the design of materials for biomedical applications.

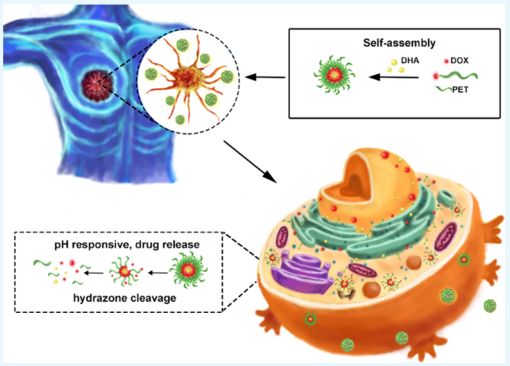

INTRODUCTION

An antitumor nanodrug delivery system (ATNDDS) may have many advantages over traditional tumor treatments. First, encapsulating antitumor drugs into nanoscale carriers can improve the solubility of hydrophobic drugs and prolong their half-life in the circulation, thus effectively improving drug availability and treatment outcome.[1−4] Second, based on the enhanced permeability and retention (EPR) effect, drug-loaded nanoparticles accumulate in the tumor, increasing their specificity and decreasing toxic side effects. In addition, different chemotherapeutic agents can be coloaded into nanoparticles to achieve a synergistic effect. Carriers for nanodrug delivery systems commonly consist of liposomes, micelles, inorganic nanoparticles, or natural polymers.[5] Compared with other compounds, natural polysaccharides can be obtained from a variety of different sources possessing excellent properties regarding sustainability and environmental protection. Natural polymers used as nanocarriers include chitosan, sodium alginate, pectin, and others. Of these polysaccharides, compared with other commonly used natural environmentally friendly materials with no medicinal effects or targeting properties, pectin has unique characteristics. It is a simple, nontoxic carbohydrate rich in galactose, which cannot pass through the intestinal wall into the circulatory system.[6−12] Its most noteworthy property is that it can effectively inhibit tumor growth and metastasis. Galactose sugar chains compete with the natural ligand of galectin-3 by binding to this molecule, thus regulating specific signal transduction pathways and inhibiting tumor cell growth.[13−15] Previous work has shown that combining the small molecule pectin with the chemotherapeutic drug DOX as adjuvant therapy increases its effectiveness and reduces the toxicity of this agent.[16−19]

Nanocarriers can avoid the multidrug efflux pump action of some transporters and reduce the extrusion of drugs from the cell.[20−29] In the present study, we designed a nanoparticle carrier based on the modification of pectin and the chemotherapeutic drug DOX. The preparation of this delivery system is not complicated, and it does not need large amounts of any toxic reagents. We simultaneously loaded the nanoparticles with another anticancer drug, dihydroartemisinin (DHA), and documented synergistic effects. This work contributes to an alternative drug platform that can help control cancer. Natural diversity has developed safer and greener cancer treatments.

RESULTS AND DISCUSSION

Fabrication of PET-DOX/DHA NPs. The amphiphilic pectin/doxorubicin (PET/DOX) prodrug was prepared via multiple synthetic processes (Figure S1). As shown in Figure 1. the characteristics of PET, DOX, and PET/DOX were established by ^{1}H NMR. The detected peaks at δ 2.5−3.5 ppm are the characteristic methyl proton peaks of PET, and

Received: December 16, 2020
Accepted: January 25, 2021
Published: April 8, 2021

https://dx.doi.org/10.1021/acsomega.0c06131
ACS Omega 2021, 6, 9998−10004

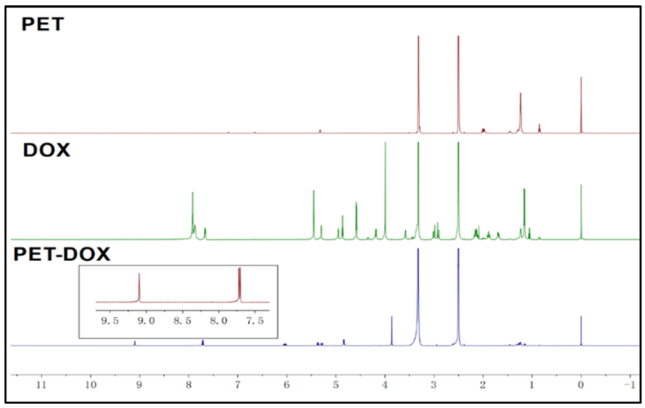

Figure 1. ^{1}H NMR spectra of PET, DOX, and PET-DOX.

those at δ 7.8−7.5 ppm are attributed to the benzene of DOX. Note that a new characteristic peak appears at δ 9.1 ppm. This new signal reflects the acyl hydrazone bond between PET and DOX, suggesting the successful synthesis of DOX and PET.

Characteristics of PET-DOX/DHA NPs. The morphology of PET/DOX-DHA nanoparticles was observed by transmission electron microscopy (TEM). Figure 2. shows that the PET/DOX-DHA nanoparticles are present in the spherical form with no agglomeration. The size of the PET/DOX-DHA particles averaged 202.6 ± 5.3 nm in an aqueous solution. Also, the amount of DOX and DHA drug-loaded into PET/DOX-DHA NPs was calculated according to the standard absorption curve (Figure S2a,b). The DLE of DOX and DHA was 11.3 and 7.8%. Based on their favorable distribution characteristics, these small-sized drug-carrying nanoparticles may be beneficial for passively targeting tumor cells and maintaining drug concentrations in the circulation for extended periods.

In Vitro Drug Release. As expected, PET-DOX/DHA NPs proved to possess excellent pH-responsive properties (Figure 3a,b). After 120 h, DOX release at pH 7.4 was only about 17.7%, much lower than 77.4% at pH 5.5. DHA also showed a similar phenomenon; after 250 h, the DHA release at pH 7.4 was only about 24.3%, much lower than 52.7% at pH 5.5. There was also no bolus release at pH 7.4. The accumulated release of DOX increased, especially at pH 5.5. This may be due to the stability of the acyl hydrazone bond between DOX and pectin in neutral or alkaline aqueous solutions; however, at lower pH, there may be a reversible chain exchange reaction.

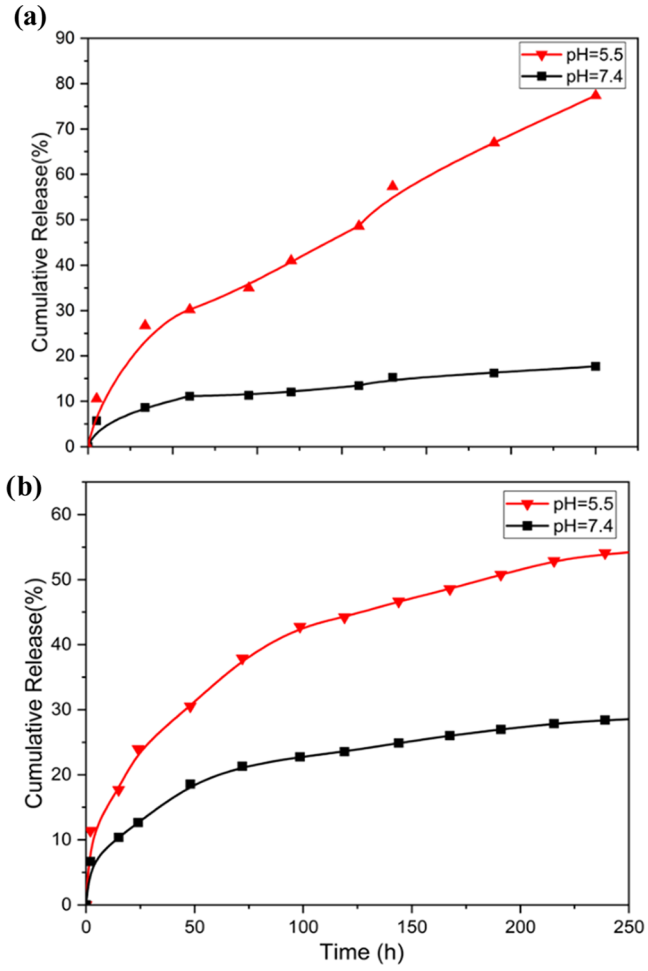

Figure 3. (a) DOX release from PET/DOX-DHA NPs under different pH conditions. (b) DHA release from PET/DOX-DHA NPs under different pH conditions.

In Vitro Cytotoxicity Assay. The cytotoxicity of PET-DOX/DHA NPs is lower than that of free DHA and DOX. This phenomenon is because the free drugs can diffuse more easily through the cell membrane. However, as shown in Figure 4b, the viability of the MCF-7 cells after incubation for

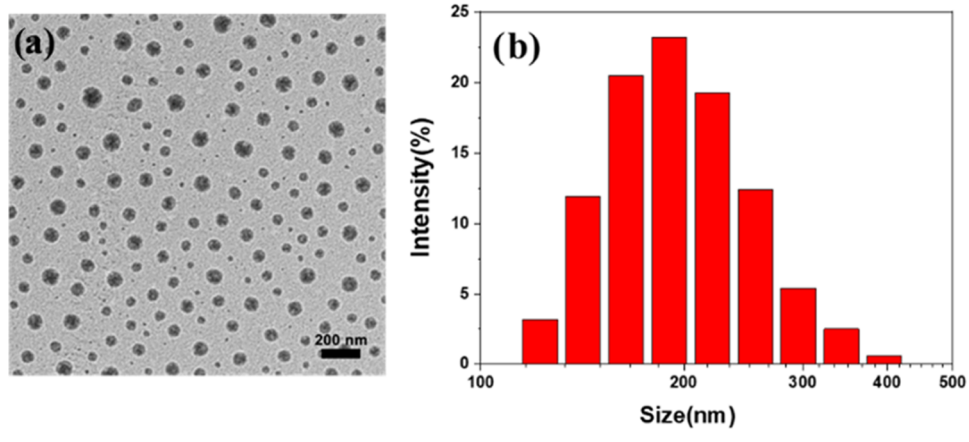

Figure 2. (a) TEM image and (b) DLS of PET-DOX/DHA.

https://dx.doi.org/10.1021/acsomega.0c06131
ACS Omega 2021, 6, 9998−10004

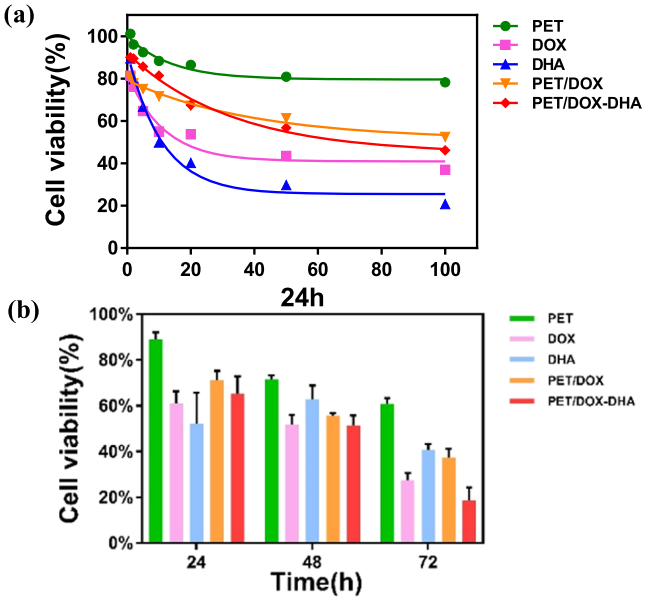

Figure 4. (a) Cell viability of MCF-7 cells treated with different concentration gradients (μg/mL) for 24 h; (b) cell viability of MCF-7 cells at 24, 48, and 72 h in different treatment groups with the same concentration.

different times at the same concentration of DOX (10 μg/mL) was lower after 72 h of PET-DOX/DHA NP treatment than with free DOX, DHA, or PET-DOX treatment. The CI of 0.83 for PET-DOX/DHA NPs suggests a marked synergistic effect. One concern is that pectin itself can inhibit breast cancer cells, supposedly by the binding of galactose in the pectin molecules with Gal3, which is overexpressed in tumor cells.

In Vitro Cellular Uptake. To confirm the intracellular location of the prepared nanoparticles, we exploited the CSLM technique, which allows a visual inspection of the cell. Figure 5a shows that free DOX accumulated in the nucleus of MCF-7 cells. Confocal images of cells incubated with PET/DOX-DHA NPs show that DOX released from these NPs accumulated in the cell nucleus and also in the cytoplasm. Flow cytometry was used to compare DOX and nanoparticle uptake into the cells. This revealed efficient cellular uptake of PET/DOX-DHA NPs, which was significantly greater than that of free DOX (Figure 5b,c)

In Vivo Antitumor Efficiency. As shown in Figure 6a,c, both groups of agents containing DOX could inhibit tumor growth in mice compared with phosphate-buffered saline (PBS) controls. In the PET/DOX-DHA NP group, tumor growth was significantly slower than in control animals. The TGI index for DOX and PET/DOX-DHA NPs is 35.02 and 55.27% (Table 1), respectively, indicating that PET/DOX-DHA NPs are more effective than the free drug. After the 10-day treatment period, the weights of tumors in the PET/DOX-DHA group were the lowest of all treatments (Figure 6b). Mice in the DOX group lost weight, probably due to its toxic side effects. Taken together, these results indicate that the nanoparticles have good biocompatibility.

CONCLUSIONS

Pectin is an edible polysaccharide, which has already been proven useful for the construction of specific drug delivery systems. However, exploiting the acyl hydrazone bond to release drugs from pectin nanoparticle constructs at lower pH has not yet been reported. In the present study, we have developed a pH-responsive nanoparticle carrier based on pectin. This platform combining DOX and also loaded with DHA releases DOX at the tumor site due to the low breaking of the acyl hydrazone bond of the nanoparticles. The size of our PET-DOX/DHA NPs was quite uniform, with an average particle size of 202 nm and drug loads of DOX and DHA of 11.3 and 7.8%. In in vitro experiments, the NPs significantly inhibited tumor cell proliferation, and the therapeutic effect was further enhanced in combination with DHA. The results suggest that PET-DOX/DHA NPs are potentially efficient platforms for the delivery of hydrophobic chemotherapeutic drugs. Thus, pectin may serve as a promising candidate for the treatment of cancer. Such natural polysaccharides have great clinical translation potential due to their simple and green preparation process.

MATERIALS AND METHODS

Materials. Pectin (PET) (55−70% esterified from citrus fruit) was obtained from Sigma (St. Louis, USA). Doxorubicin (DOX) and hydrazine hydrate ($N_2H_4{\cdot}H_2O$) were supplied by Nine-Dinn Chemistry (Shanghai) Co., Ltd. (Shanghai, China). Dihydroartemisinin (DHA) was purchased from Chengdu Pufei De Biotech Co., Ltd. (Chengdu, Sichuan, China). Dimethyl sulfoxide (DMSO) was produced by Shanghai Aladdin Biochemical Technology Co., Ltd., and RPMI-1640 medium, fetal bovine serum (FBS), penicillin−streptomycin, and trypsin-EDTA were bought from Gibco Co. The Cell-Counting Kit-8 (CCK-8) was supplied by Dojindo Laboratories (Japan). All other reagents were purchased from Sigma-Aldrich. MCF-7 breast cancer and 4T1 breast cancer cell lines were donated by the Institute of Process Engineering, Chinese Academy of Sciences (Beijing, China). Female BALB/c mice, 6−8 weeks of age, were purchased from Peking University Laboratory Animal Center (Beijing, China). All animal experiments were performed according to the Guide for the Care and Use of Laboratory Animals and approved by the Experimental Animal Ethics Committee, Beijing.

Preparation of Nanoparticles. PET (50 mg) was dissolved in deionized water at 50 °C for 30 min. Next, 3 mL of $N_2H_4{\cdot}H_2O$ was added to the mixture with stirring at room temperature. After 16 h, 20 mg of DOX dissolved in a small amount of dry DMSO was added to the mixture for 24 h. The mixture was transferred to a dialysis bag (3500 MWCO) and dialyzed for 24 h, and the PET-DOX conjugates were obtained after lyophilization.[25]

PET-DOX/DHA nanoparticles were generated by self-assembly, as described previously. We dissolved 10 mL of the PET-DOX solution, with vigorous stirring over 5 min. Afterward, the solution was dialyzed again in a 3500 MWCO dialysis bag against deionized water for 24 h. After freeze-drying, the drug-loaded nanoparticles PET-DOX/DHA were collected.

Characterization of the Nanoparticles. The chemical bonds of the nanoparticles were identified by NMR spectroscopy. The morphology of the self-assembled prodrug nanoparticles was investigated by transmission electron microscopy. The PET/DOX-DHA nanomicelles were dropped onto a clean copper net by the suspension method and then dried in air. The size and distribution of PET/DOX-DHA NPs were confirmed by dynamic light scattering. The freeze-dried sample of PET/DOX-DHA was dissolved in deionized water and measured at room temperature.

https://dx.doi.org/10.1021/acsomega.0c06131
ACS Omega 2021, 6, 9998−10004

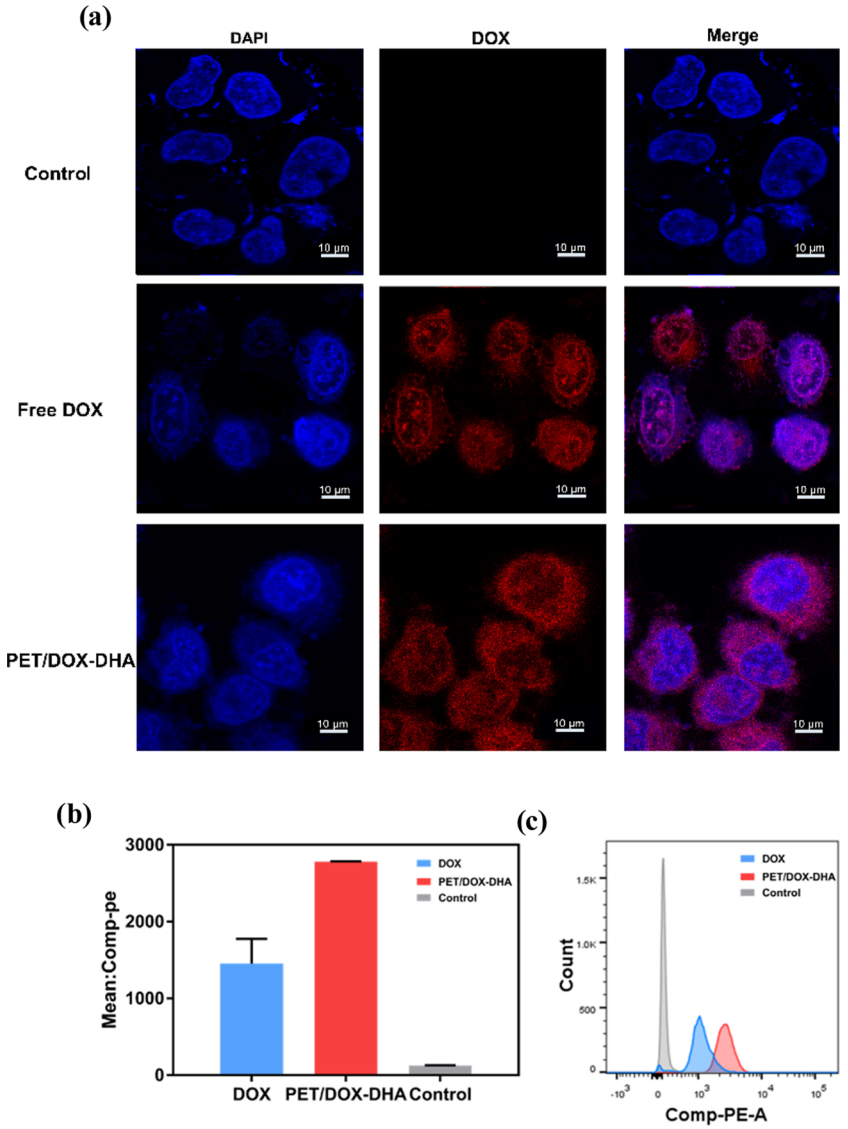

Figure 5. (a) Laser confocal images of control, free DOX, and PET/DOX-DHA NPs. (b) Histogram analysis and (c) mean fluorescence intensity of cellular uptake of DOX and PET/DOX-DHA NPs.

Determination of Drug Loading Efficiency and Encapsulation Efficiency. To study the drug loading efficiency (DLE) of PET/DOX-DHA nanoparticles, the amount of DOX contained in it was determined by ultraviolet spectrophotometry, and DHA was analyzed by high-performance liquid chromatography (HPLC). To this end, 10 mg of the PET/DOX-DHA nanoparticle powder was dissolved in 5 mL of DMSO, and the UV detection wavelength of the spectrometer was set at 480 nm. The HPLC method employed acetonitrile/H_2O (60/40), at a flow rate of 1 mL/min, column temperature of 25 °C, and detection wavelength of 210 nm. Each sample was tested 3 times in parallel. The DLE of DOX and DHA was calculated according to the standard absorption curve. The formula for calculating DLE (%) is as follows: DLE (wt %) = $m_A/M \times 100\%$, where m_A is the weight of the DOX or DHA drug (mg), and M is the total weight of the polymer (mg).

In Vitro Release. The release of DOX from PET/DOX-DHA NPs was monitored by a dialysis method. PET/DOX-DHA powder (3 mg) was dissolved in 3 mL of deionized water and then placed in dialysis bags; the analysis was carried out under conditions simulating normal tissue (pH = 7.4), as well as in an acidic environment (pH = 5.5). To further improve the stability of hydrophobic drugs in the medium, 0.1% (W/V) Tween 80 was added. The temperature was maintained at 37 ± 0.5 °C, and 1 mL of the medium was taken out at predetermined time intervals. Subsequently, an equal volume of fresh medium at the same temperature and pH was added. The cumulative DOX release rate R (%) from the PET/DOX-DHA nanoparticles was determined by UV spectrometry and that of DHA by HPLC. The experiment was repeated 3 times and the results were averaged as follows: R (%) = $(\sum_1^{m-1} C_i V_i + C_m V_m)/M$, where R is the cumulative release rate of the drug (%), M is the mass of nanoparticles (μg), V_m is the total volume (mL), C_m is the concentration of the drug at the mth order (g/mL), V_i is the volume of the sample at the ith order (mL), and C_i is the concentration at the ith order (g/mL).

In Vitro Cytotoxicity Assay. We used the CCK-8 kit to investigate the cellular cytotoxicity of the drug. Sample solutions (PET, DOX, DHA, PET/DOX, and PET/DOX-DHA) at different concentrations were added to 96-well plates containing 4×10^3 cells per well and incubated for 24, 48, or

https://dx.doi.org/10.1021/acsomega.0c06131
ACS Omega 2021, 6, 9998−10004

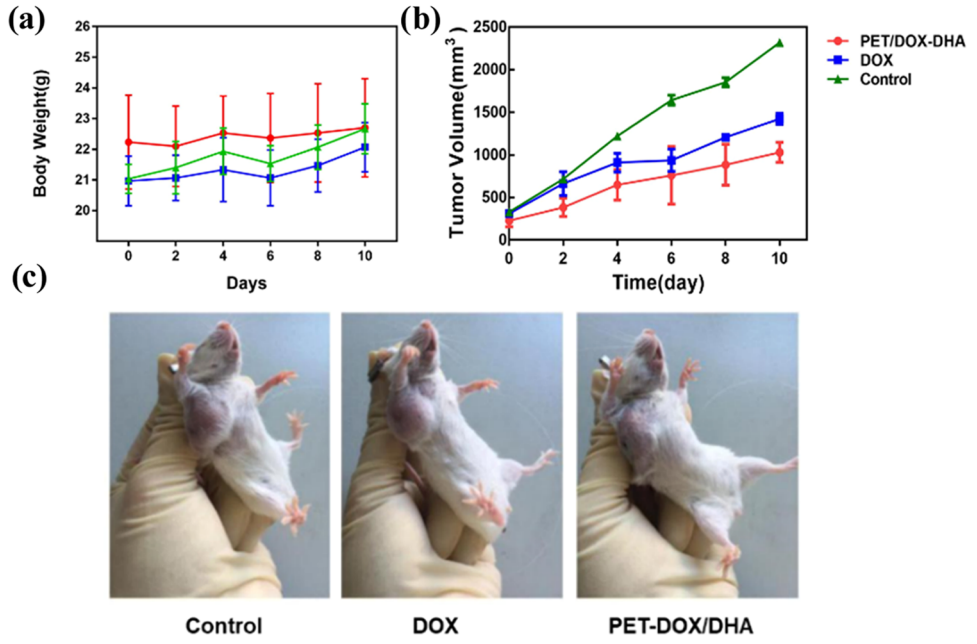

Figure 6. (a) Changes in the body weight of tumor-bearing mice in different experimental groups; (b) body weight changes in different model groups. (c) Photographs of tumors from different groups on day 10.

Table 1. In Vivo Antitumor Efficacy at Day 10

group	mean TV ± SD	RTV	TGI (%)
control	2320.48 ± 37.98	7.70 ± 0.98	
DOX	1424.87 ± 64.06	5.01 ± 0.67	35.02
PET/DOX-DHA	1031.16 ± 77.37	3.45 ± 0.60	55.27

72 h. A 50 μL mixture of CCK-8 with complete culture medium was added to each well and incubated for 2 h in the dark. Cell viability was measured at 450 nm as follows: Cell viability = $(A_{control} - A_{sample})/A_{control} \times 100\%$, where $A_{control}$ refers to the absorbance of the blank group, A_{sample} refers to the absorbance of the administration group, and synergy index (CI) = $(DOX_{combined}/DOX_{single}) + (DHA_{combined}/DHA_{single})$. CI < 1 indicates a synergistic interaction between the drugs, CI = 1 indicates an additive effect, and CI > 1 indicates an antagonism between the drugs.

Cellular Uptake of Nanoparticles. The uptake of PET/DOX-DHA and DOX by human breast cancer MCF-7 cells was investigated by flow cytometry and laser confocal microscopy. MCF-7 cells were cultured in a six-well plate at 20×10^5 cells per well at 37 °C for 24 h. Then 0.2 mL of DOX and PET/DOX-DHA nanoparticles at equal concentrations were added to the wells, and the plates were incubated at 37 °C for 4 h. DPBS buffer at pH 7.4 was then used to detach and wash the cells, after which they were resuspended in DPBS and analyzed by flow cytometry.

To visualize the uptake of material into cells, we adopted the confocal laser method. The cells were placed in a culture dish at 40×10^5 cells per dish. DOX and PET/DOX-DHA nanoparticles at equal concentrations were added and coincubated with the cells for 4 h. The culture medium was discarded, and the cells were washed with DPBS three times. The cells were then fixed with 4% paraformaldehyde for 15 min followed by DAPI staining in the dark for 15 min. The DAPI stain was then discarded, and the cells were washed three times with DPBS. Finally, 2 mL of DPBS was added and the uptake of PET/DOX-DHA and DOX by MCF-7 cells was investigated under 488 nm excitation.

In Vivo Antitumor Activity. MCF-7 cells (2×10^5 cell/mouse) were injected into female C57BL/6 mice (6−7 weeks old) to establish xenografts of individual tumors. When the average tumor volume reached 100−150 mm^3, the mice were randomly divided into three groups (n = 6/group) as follows: PBS (control group), DOX (10 mg/kg), and PET/DOX-DHA (DOX equivalent concentration 10 mg/kg). Drugs were administered through the caudal vein, followed by intravenous injection every three days. Tumor size and body weight were monitored every other day. After completion of the experiment (2 weeks), mice were sacrificed by cervical dislocation. Tumor tissue was dissected and weighed under sterile conditions. The tumor volume was calculated as follows: Tumor volume (TV) = (length × width^2)/2; relative tumor volume (RTV) = TV/TV^0, where TV^0 refers to body weight before treatment; and Tumor growth inhibition percentage (% TGI) = (C − T)/C × 100%, where C and T represent the average tumor volume of the control and treatment groups, respectively.

■ ASSOCIATED CONTENT

Supporting Information

The Supporting Information is available free of charge at https://pubs.acs.org/doi/10.1021/acsomega.0c06131.

Synthetic route of PET/DOX conjugation and the standard curve of DOX and DHA (PDF)

■ AUTHOR INFORMATION

Corresponding Authors

Jiandu Lei − *Beijing Key Laboratory of Lignocellulosic Chemistry, College of Material Science and Technology, Beijing Forestry University, Beijing 100083, P. R. China;* orcid.org/0000-0002-1432-0588; Email: ljd2012@bjfu.edu.cn

Luying Wang − *Beijing Key Laboratory of Lignocellulosic Chemistry, College of Material Science and Technology,*

https://dx.doi.org/10.1021/acsomega.0c06131
ACS Omega 2021, 6, 9998−10004

Beijing Forestry University, Beijing 100083, P. R. China; Email: wangly@bjfu.edu.cn

Authors

Yinghua Tao − *Beijing Key Laboratory of Lignocellulosic Chemistry, College of Material Science and Technology, Beijing Forestry University, Beijing 100083, P. R. China; Westlake University, Hangzhou 310024, P. R. China;* orcid.org/0000-0001-8452-962X

Dan Zheng − *Beijing Key Laboratory of Lignocellulosic Chemistry, College of Material Science and Technology, Beijing Forestry University, Beijing 100083, P. R. China*

Jingyang Zhao − *Beijing Key Laboratory of Lignocellulosic Chemistry, College of Material Science and Technology, Beijing Forestry University, Beijing 100083, P. R. China*

Kefeng Liu − *Beijing Key Laboratory of Lignocellulosic Chemistry, College of Material Science and Technology, Beijing Forestry University, Beijing 100083, P. R. China; State Key Laboratory of Biobased Material and Green Papermaking, Qilu University of Technology (Shandong Academy of Sciences), Jinan 250353, Shandong, P. R. China*

Jing Liu − *Beijing Key Laboratory of Lignocellulosic Chemistry, College of Material Science and Technology, Beijing Forestry University, Beijing 100083, P. R. China*

Complete contact information is available at: https://pubs.acs.org/10.1021/acsomega.0c06131

Author Contributions

This manuscript was written through contributions from all authors. All authors have given approval to the final version of the manuscript.

Funding

This study was supported by the National Key R&D Program of China [No. 2019YFB1309703], the National Natural Science Foundation of China [No. 21978024], and Beijing Natural Science Foundation [No. 2202034].

Notes

The authors declare no competing financial interest.

■ ACKNOWLEDGMENTS

The authors would like to gratefully acknowledge the Institute of Process Engineering of China Academy of Science, Peking University Laboratory Animal Center, for technical support.

■ REFERENCES

(1) Faraji, A. H.; Wipf, P. Nanoparticles in cellular drug delivery. *Bioorg. Med. Chem.* **2009**, *17*, 2950−2962.

(2) Kumaresh; Soppimath; Tejraj; Aminabhavi; Anandrao. Biodegradable polymeric nanoparticles as drug delivery devices. *J. Control. Release.* **2001**, *70*, 1−20.

(3) Lee, B. K.; Yun, Y. H.; Park, K. Smart nanoparticles for drug delivery: Boundaries and opportunities. *Chem. Eng. Sci.* **2015**, *125*, 158−164.

(4) Duncan, R.; Richardson, S. C. Endocytosis and intracellular trafficking as gateways for nanomedicine delivery: opportunities and challenges. *Mol. Pharmacol.* **2012**, *9*, 2380−2402.

(5) Cho, K.; Wang, X.; Nie, S.; Chen, Z. G.; Shin, D. M. Therapeutic nanoparticles for drug delivery in cancer. *Clin. Cancer Res.* **2008**, *14*, 1310−1316.

(6) Jiang, J.; Eliaz, I.; Sliva, D. Synergistic and additive effects of modified citrus pectin with two polybotanical compounds, in the suppression of invasive behavior of human breast and prostate cancer cells. *Integr. Cancer Ther.* **2013**, *12*, 145−152.

(7) Kim, C. C.; Healey, G. R.; Kelly, W. J.; Patchett, M. L.; Jordens, Z.; Tannock, G. W.; Sims, I. M.; Bell, T. J.; Hedderley, D.; Henrissat, B.; Rosendale, D. I. Genomic insights from Monoglobus pectinilyticus: a pectin-degrading specialist bacterium in the human colon. *ISME J.* **2019**, *13*, 1437−1456.

(8) Li, W.; Zhang, K.; Yang, H. Pectin Alleviates High Fat (Lard) Diet-Induced Nonalcoholic Fatty Liver Disease in Mice: Possible Role of Short-Chain Fatty Acids and Gut Microbiota Regulated by Pectin. *J. Agric. Food Chem.* **2018**, *66*, 8015−8025.

(9) Maxwell, E. G.; Belshaw, N. J.; Waldron, K. W.; Morris, V. J. Pectin − An emerging new bioactive food polysaccharide. *Trends Food Sci. Technol.* **2012**, *24*, 64−73.

(10) Jackson, C. L.; Dreaden, T. M.; Theobald, L. K.; Tran, N. M.; Beal, T. L.; Eid, M.; Gao, M. Y.; Shirley, R. B.; Stoffel, M. T.; Kumar, M. V.; Mohnen, D. Pectin induces apoptosis in human prostate cancer cells: correlation of apoptotic function with pectin structure. *Glycobiology* **2007**, *17*, 805−819.

(11) Prado, S. B. R.; Beukema, M.; Jermendi, E.; Schols, H. A.; de Vos, P.; Fabi, J. P. Pectin Interaction with Immune Receptors is Modulated by Ripening Process in Papayas. *Sci. Rep.* **2020**, *10*, No. 1690.

(12) Tian, L. J.; Singh, A.; Singh, A. V. Synthesis and characterization of pectin-chitosan conjugate for biomedical application. *Int. J. Biol. Macromol.* **2020**, *153*, 533−538.

(13) Funasaka, T.; Raz, A.; Nangia-Makker, P. Nuclear transport of galectin-3 and its therapeutic implications. *Semin. Cancer Biol.* **2014**, *27*, 30−38.

(14) Gunning, A. P.; Bongaerts, R. J.; Morris, V. J. Recognition of galactan components of pectin by galectin-3. *FASEB J.* **2009**, *23*, 415−424.

(15) Huang, P.-H.; Fu, L.-C.; Huang, C.-S.; Wang, Y.-T.; Wu, M.-C. The uptake of oligogalacturonide and its effect on growth inhibition, lactate dehydrogenase activity and galactin-3 release of human cancer cells. *Food Chem.* **2012**, *132*, 1987−1995.

(16) Bai, F.; Diao, J.; Wang, Y.; Sun, S.; Zhang, H.; Liu, Y.; Wang, Y.; Cao, J. A New Water-Soluble Nanomicelle Formed through Self-Assembly of Pectin-Curcumin Conjugates: Preparation, Characterization, and Anticancer Activity Evaluation. *J. Agric. Food Chem.* **2017**, *65*, 6840−6847.

(17) Delphi, L.; Sepehri, H. Apple pectin: A natural source for cancer suppression in 4T1 breast cancer cells in vitro and express p53 in mouse bearing 4T1 cancer tumors, in vivo. *Biomed. Pharmacother.* **2016**, *84*, 637−644.

(18) Eliaz, I.; Raz, A. Pleiotropic Effects of Modified Citrus Pectin. *Nutrients* **2019**, *11*, No. 2619.

(19) Hussien, N. A.; Isiklan, N.; Turk, M. Pectin-conjugated magnetic graphene oxide nanohybrid as a novel drug carrier for paclitaxel delivery. *Artif. Cells, Nanomed., Biotechnol.* **2018**, *46*, 264−273.

(20) Chen, Y.; Su, M.; Li, Y.; Gao, J.; Zhang, C.; Cao, Z.; Zhou, J.; Liu, J.; Jiang, Z. Enzymatic PEG-Poly(amine-co-disulfide ester) Nanoparticles as pH- and Redox-Responsive Drug Nanocarriers for Efficient Antitumor Treatment. *ACS Appl. Mater. Interfaces* **2017**, *9*, 30519−30535.

(21) Dong, S.; Sun, Y.; Liu, J.; Li, L.; He, J.; Zhang, M.; Ni, P. Multifunctional Polymeric Prodrug with Simultaneous Conjugating Camptothecin and Doxorubicin for pH/Reduction Dual-Responsive Drug Delivery. *ACS Appl. Mater. Interfaces* **2019**, *11*, 8740−8748.

(22) Gao, W.; Chan, J. M.; Farokhzad, O. C. pH-Responsive Nanoparticles for Drug Delivery. *Mol. Pharm.* **2010**, *7*, 1913−1920.

(23) Hou, S.; Chen, S.; Dong, Y.; Gao, S.; Zhu, B.; Lu, Q. Biodegradable Cyclomatrix Polyphosphazene Nanoparticles: A Novel pH-Responsive Drug Self-Framed Delivery System. *ACS Appl. Mater. Interfaces* **2018**, *10*, 25983−25993.

(24) Javanbakht, S.; Saboury, A.; Shaabani, A.; Mohammadi, R.; Ghorbani, M. Doxorubicin Imprinted Photoluminescent Polymer as a pH-Responsive Nanocarrier. *ACS Appl. Bio Mater.* **2020**, *3*, 4168−4178.

(25) Kim, T.-H.; Jeong, G.-W.; Nah, J.-W. Preparation and anticancer effect of transferrin-modified pH-sensitive polymeric drug nanoparticle for targeted cancer therapy. *J. Ind. Eng. Chem.* **2017**, *54*, 298−303.
(26) Li, M.; Sun, X.; Zhang, N.; Wang, W.; Yang, Y.; Jia, H.; Liu, W. NIR-Activated Polydopamine-Coated Carrier-Free "Nanobomb" for In Situ On-Demand Drug Release. *Adv. Sci.* **2018**, *5*, No. 1800155.
(27) Liu, S.; Ono, R. J.; Yang, C.; Gao, S.; Ming Tan, J. Y.; Hedrick, J. L.; Yang, Y. Y. Dual pH-Responsive Shell-Cleavable Polycarbonate Micellar Nanoparticles for in Vivo Anticancer Drug Delivery. *ACS Appl. Mater. Interfaces* **2018**, *10*, 19355−19364.
(28) Liu, Y.; Qiao, L.; Zhang, S.; Wan, G.; Chen, B.; Zhou, P.; Zhang, N.; Wang, Y. Dual pH-responsive multifunctional nanoparticles for targeted treatment of breast cancer by combining immunotherapy and chemotherapy. *Acta Biomater.* **2018**, *66*, 310−324.
(29) Chen, D.; Tang, Q.; Zou, J.; Yang, X.; Huang, W.; Zhang, Q.; Shao, J.; Dong, X. pH-Responsive PEG-Doxorubicin-Encapsulated Aza-BODIPY Nanotheranostic Agent for Imaging-Guided Synergistic Cancer Therapy. *Adv. Healthcare Mater.* **2018**, *7*, No. e1701272.

https://dx.doi.org/10.1021/acsomega.0c06131
ACS Omega 2021, 6, 9998−10004